European Journal of Ophthalmology / Vol. 17 no. 3, 2007 / pp. 377-382

Optic nerve alterations in P27^{Kip1} knockout mice

E. LOPEZ-SANCHEZ[1], E. FRANCES-MUÑOZ[2], V. CHAQUES[1], M.L. SANCHEZ-BENAVENT[1], J.L. MENEZO[2]

[1]Hospital Arnau de Vilanova, Valencia
[2]Hospital "La Fe", Valencia - Spain

PURPOSE. *To study the morphologic characteristics of the optic nerve (ON) by using an experimental model of knockout mice for the expression of the P27^{Kip1} gene, mainly involved in cell cycle arrest, apoptosis control, and retinoblastoma protein phosphorylation.*
METHODS. *Eyeballs with the retrobulbar ON attached were obtained from 26-week-old mice. By using morphologic and morphometric techniques, light and electron transmission microscopy, the ON characteristics were determined in two groups of mice: 1) wild type mice as the control group (n=15), 2) homozygous knockout mice (-/-) for the P27^{Kip1} gene as the knockout group (n=15). Glial fibrillary acidic protein (GFAP) and myelin basic protein (MBP) were studied using Western blot and immunoblotting approaches.*
RESULTS. *The ON cross-sectional area was significantly larger in the P27^{Kip1} knockout mice group than in the control group ($p<0.001$). The axon sizes in knockout animals were much larger than in wild-type mice ($p<0.001$). Higher number of axons forming the ON, intra-axonal degeneration, myelin sheath, and axoplasm density alterations were found in P27^{Kip1} knockout mice when compared with control group ($p<0.001$). Analysis of lysates of optic nerves by Western blot showed less expression of myelin basic protein and GFAP in P27^{Kip1} knockout mice as compared to wild type mice ($p<0.005$, $p<0.01$, respectively).*
CONCLUSIONS. *The morphologic and morphometric results suggest that homozygous P27^{Kip1} knockout mice had hypertrophic, hyperplastic, and dystrophic ON. (Eur J Ophthalmol 2007; 17: 377-82)*

KEY WORDS. *Knockout, Morphology, Morphometry, Optic nerve, P27^{Kip1}*

Accepted: November 5, 2006

INTRODUCTION

Progression through or exit from the eukaryotic cell division cycle is regulated by a series of stringent control mechanisms.
Retinoblastoma protein (Rb) phosphorylation is thought to play a central role in the cell cycle control (1, 2). Its phosphorylation is regulated by cyclins and their partners, the cyclin-dependent kinases. Mammalian cell cycle requires the activation of cyclin-dependent kinases (CDKs) through their association with regulatory subunits called cyclins. Different CDKs/cyclin holoenzymes are activated at specific phases of the cell cycle (3). The active CDK/cyclin complex phosphorylates the retinoblastoma gene product and the related pocket proteins p107 and p130 from the G1 cell cycle phase to mitosis, which in turn regulates the activity of members of the E2F family of transcription factors (4). Cell proliferation in mammals is negatively regulated by CDK inhibitory proteins (CKIs) that bind to the CDK/cyclin holoenzymes and inhibit their activity. CKIs of the CIP/KIP family (p21, p27, and p57) bind to and inactivate a broad range of CDKs (5, 6).
P27^{Kip1} null mice showed increased body weight, multiorgan hyperplasia, luteal cell proliferation, testicular and ovarian hyperplasia (7), strikingly enlarged thymus (8), and as in RbP +/- mice (9), pituitary tumors (7). Regarding the

 1120-6721/377-06$15.00/0

ophthalmologic area, P27^{Kip1} deficient mice exhibit an increase in the number of mitotic cells throughout development as well as extensive apoptosis, particularly during the latter stages of retinal histogenesis (10). P27^{Kip1} deficient retinas appear to have a normal size; however, they show a marked disorganization of the cellular pattern, though in a partially penetrating fashion, with patches of the outer nuclear layer invading the rod and cone layer until they reach the pigment epithelium. The electroretinograms of these mutant mice showed an approximately twofold reduction in their amplitudes (7).

Although our knowledge about P27 gene function in the optic nerve is not comprehensive, we know that P27^{Kip1} is an important component of the oligodendrocyte progenitor cell decision to withdraw from the cell cycle (11), which contributes to the oligodendrocyte differentiation by regulating the transcription of the myelin basic protein gene (12). On the contrary, oligodendrocyte progenitor cell differentiation is perturbed in the absence of cyclin-dependent kinase inhibitor P27^{Kip1} (11).

The function of P27^{Kip1} in the retina and ON is far from completely understood. P27^{Kip1} experimental models may provide ophthalmologists a chance to study the molecular basis involved in ocular oncology or neurodegenerative processes.

In the present work, the optic nerves from homozygous knockout P27^{Kip1} mice were processed for light and electron transmission microscopes, and morphologic and morphometric analyses were performed.

METHODS

Animals and experimental design

All experiments were performed in accordance with EC Regulation (November 1986). Normal and homozygous (C57BL/6) P27^{Kip1} mutant mice (P27^{Kip1} -/-) were used. Mice were maintained in a laboratory room illuminated from 7 AM to 7 PM, in standard conditions of temperature and humidity. Two study groups were established: 1) 15 26-week-old wild type mice (15 males) as the control group, 2) 15 26-week-old mutant homozygotes (P27^{Kip1} -/-) (15 males) as the knockout group. They all had free access to food and water. The groups were fed with standard diet (Purina). Mice were classified and maintained in cages during the whole experiment until euthanasia (previously anesthetized with ether).

Morphologic and morphometric analysis

Light microscopy. The right eyes and optic nerves were enucleated and the optic nerves sectioned 1 to 3 mm behind the eyeball. Samples were fixed in 2% glutaraldehyde and 3% glutaraldehyde in 0.1 M cacodylate buffer (pH 7.4). Standard dehydration of the samples was performed by embedding in epoxy resin (EPON 850). Semithin sections (1 µm) were cut on an ultramicrotome LKB. Sections were stained with 2% toluidine blue and examined using a light microscopy (Leika) with image analysis system (Q-win). To assess the morphometric analysis of the ON, digital micrographs were taken, as reported by Pinazo-Durán et al (13). The ON cross-areas were measured (Scion image, Scion Corporation, PC WindowsXP), excluding meningeal covering.

Transmission electron microscopy (TEM). Eyes were first examined under light microscopy to determine areas of interest. Ultrathin sections of approximately 100 nm were then cut and collected on copper grids. Sections were stained with 4% uranyl acetate and lead citrate. Ultrathin sections were then evaluated by TEM and photographed at ×12,000 and ×25,000 magnification.

Axonal area measurement. The axonal cross-areas were measured (Scion image). In general, 453 axons from a 700 µm^2 area in the control group and 364 from the same area in the knockout group were analyzed.

Total number of axons forming the ON. By using the ON cross-sectional area measurement and the axonal count, an estimation of the total number of axons of the ON was calculated.

Myelin sheath and axonal degeneration recording. We counted the number of normal/impaired axons in the electron micrographs with similar magnification and study area obtained from the two groups. The total number of axons studied both in the control group and in the knockout mice was 450. Breaks and disorganized myelin sheaths, and swelling, vacuolation, and inclusion bodies in the axoplasm were considered as signs of impaired myelin or axons. The number of impaired axons and myelin was expressed as a percentage of the total number of counted axons.

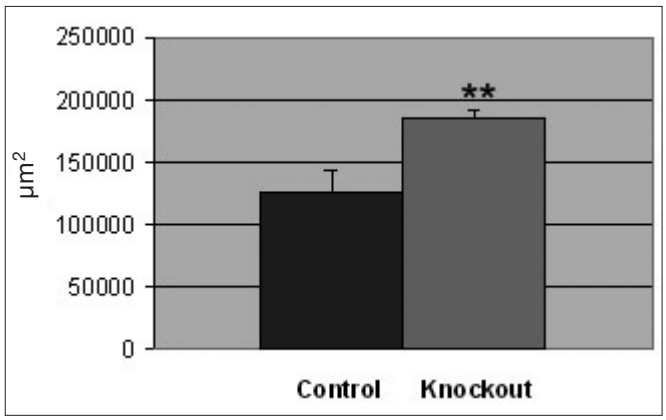

Fig. 1 - *Optic nerve cross-sectional areas: semithin sections were examined using light microscopy. Mean cross-sectional areas were larger in the knockout mice (n=15) than controls (n=15) (µm²) (p<0.01).*

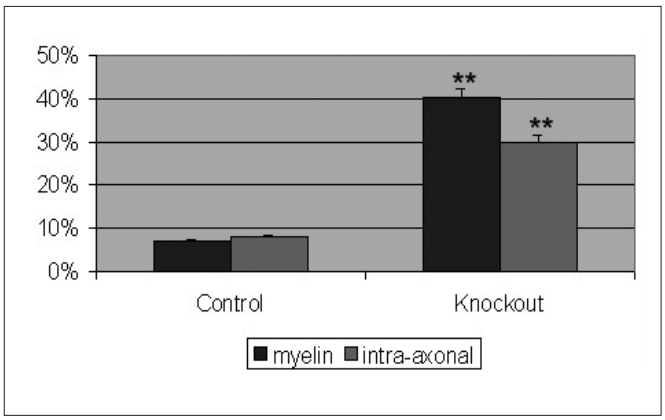

Fig. 2 - *Myelin sheath and intra-axonal degeneration: using transmission electron microscopy the total number of axons studied both in the control group and in the knockout mice was 450. The percentage of axons with profiles of myelin sheath and intra-axonal degeneration was higher in the knockout mice than in the control group (p<0.001).*

Densitometry of the axoplasmic material I- In order to assess the possible differences regarding the electron density axoplasms in both groups, we performed a densitometric analysis (Scion image) comparing 100 axons from both groups (control and knockout group). A significant decrease in the electron density axoplasm material was considered as a sign of impaired axon.

The myelination index

The myelination index is expressed as the difference between the myelin thickness and the axon diameter. The results were assembled in three different subgroups depending on the axon diameter, as we previously described (14). The first subgroup was formed by axons with a mean diameter <1 µm (SG1), the second subgroup with an axon diameter between 1 µm and 1.7 µm (SG2), the third subgroup with an axon diameter >1.7 µm (SG3).

Western blot analysis

The left optic nerves were cryopreserved (–85 ºC) until the Western blot and immunoblotting techniques were performed, as described before (15). The total number of optic nerves studied both in the control group and in the knockout mice was 15. Lysates were resolved on 12.5% Nu-PAGE gels and transferred to nitrocellulose membranes (Millipore, Bedford, MA). Membranes were probed with antibody against glial fibrillary acidic protein (GFAP) and myelin basic protein (MBP), which are elemental structural proteins of the optic nerves. Densitometric studies of the membranes were then performed.

Statistical analysis

Data were subjected to statistical analysis with SPSS, 11.5 version. Student's *t*-test and comparison of proportions were performed.

RESULTS

ON morphometric study

Data of the ON cross-sectional area are shown in Fig. 1 (results are expressed as the mean ± SE). Mean cross-sectional areas were larger in the knockout group than in the control group (125.209 μm^2 ± 17.277 versus 185.110 μm^2 ± 6.402, p<0.01).

The axonal cross-sectional areas obtained from the TEM photographs revealed higher values for the axons of the knockout mice when compared with the control group (0.8 μm^2 ± 0.95 versus 1.46 μm^2 ± 1.74, p<0.01).

In the estimation of the total number of axons within the ON, the knockout mice showed a higher number of axonal profiles than the control mice (81.028±129 versus 90.439±582) with a statistically significant difference (p<0.001).

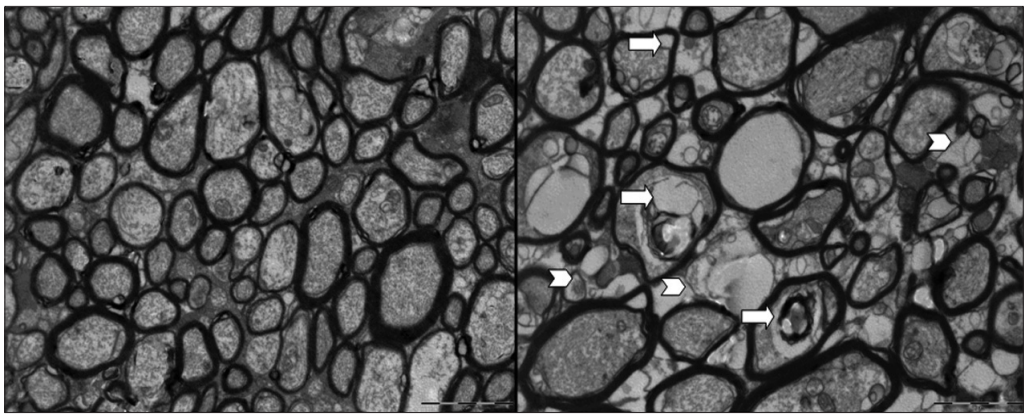

Fig. 3 - (Left) *Axons corresponding to the control group with no alteration in the morphology, intra-axonal density, or myelin.* **(Right)** *Axons corresponding to the knockout group with abundant intra-axonal degeneration profiles like axoplasma vacuolation (arrow), myelin alteration (arrowheads). A larger size of the axons is also documented. Ultrathin 100 nm.*

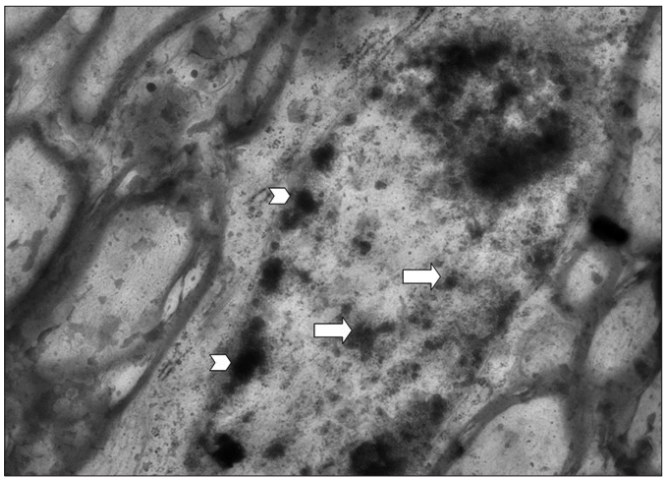

Fig. 4 - *Astrocyte nuclei with apoptotic transmission electron microscope profile: chromatin condensation (arrows) and apoptotic bodies (arrowheads). Ultrathin 100 nm.*

Morphologic study

Myelin sheath degeneration. A higher number of axons with myelin sheath alterations was found in P27^{Kip1} knockout mice when compared with the control group. The percentage of axons with profiles of myelin sheath degeneration was 6.9% in controls and 30% in the knockout mice (Fig. 2). The statistical analysis demonstrated a statistically significant difference between the two groups (comparison-of-proportions test, $p<0.001$).

The axonal degeneration signs like swelling, vacuolation and inclusion bodies were examined using TEM (Fig. 3). A higher number of axons with degeneration signs was found in P27^{Kip1} knockout mice when compared with the control group. The percentage of axons with myelin sheath degeneration was 8.09% in the control group and 40.23% in the knockout mice (Fig. 2). The statistical analysis using the comparison-of-proportions test showed a significant difference ($p<0.001$) between the two groups.

In the samples we also found apoptotic profiles in the macroglial cell nuclei, like chromatin condensation and the presence of apoptotic bodies (Fig. 4).

Densitometry of the axoplasmic material. Quantification by densitometry demonstrated in the knockout group a significant decrease in the axoplasms electron density when compared with controls (paired *t*-test, $p<0.001$).

The myelination index was lower in the knockout group than in control optic nerves. A statistically significant difference was found when comparing controls with mutant mice in the SG1, SG2, and SG3 subgroups (Student's *t*-test, $p<0.001$).

Western blot analysis. The transference to nitrocellulose membranes and incubation of the antibodies showed important differences in the band expression of the MBP and GFAP. Quantification by densitometry of those proteins expression found a lower value in terms of densitometric units in the knockout group when compared with control group (paired *t*-test, $p<0.001$) (Fig. 5).

DISCUSSION

A wide range of disorders affecting the P27 mutant mice have been described (7-10). We have attempted to characterize the ON in genetically targeted P27^{Kip1}-/- mice using morphologic and morphometric approaches. This is a preliminary step for further programmed research about

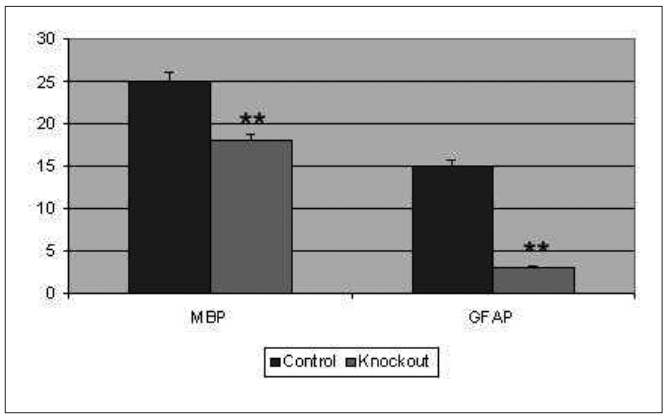

Fig. 5 - *Western blot analysis: band expression quantification by densitometry from 15 optic nerve lysates both in the control and knockout group, for the myelin basic protein and glial fibrillary acidic protein, showed a lower value in terms of densitometric units in the mutant group when compared with control group (p<0.001).*

the role of P27 gene in the pathogenic mechanisms of retinal and ON diseases.

As described herein, statistically significant quantitative differences in ON and axonal areas size, and in the number of axons conforming the ON, were found when comparing with the control ON. Apoptotic profiles in the macroglial cells and pattering disorganization in the myelin structure or intra-axonal degeneration were present. Furthermore, impairment of the GFAP or MBP expression could be demonstrated. Overall, our results strongly suggest that $P27^{Kip1}$ -/- mice show an ON hypertrophy pattern with cytoarchitectural alterations and hyperplasia.

The presence of hyperplastic axons can be explained by the theory which regards the nervous system as a tissue where progenitor cells are mitotic and cycle vigorously, but then the cell cycle stops, leading to a postmitotic state in which many cells are destined to die by programmed cell death. Finally, the surviving cells become mature, but they still remain in a quiescent G1 cell cycle phase. Consistent with the abundance of $P27^{Kip1}$ in this tissue and the function of this protein in the cell cycle is the abnormality observed in $P27^{Kip1}$ knockout mice which involves the presence of hyperplastic axons by inducing the cell to move from the G1 phase to mitosis (11, 16).

Regarding the myelination in P27-deficient ON nerves, it is known that $P27^{Kip1}$ enhances MBP gene promoter activity. P27 plays a role in the transcriptional regulation of the oligodendrocyte differentiation markers indicating that $P27^{Kip1}$ can modulate the expression of the MBP gene (12, 17, 18), with its protein being a specific marker for correct maturation and functioning oligodendrocytes. On the contrary, it would be logical to think that the absence of the P27 expression is a cause of the myelination process alteration, and this is also supported by our findings of low MBP levels detected in the Western blot analysis.

On the other hand, Casaccia-Bonnefil et al (11) suggested that the axons formed in $P27^{Kip1}$ -/- mice were normal regarding the myelination, but they found apoptotic cells in electron micrographs from the 6-day-old mice. This observation would be compatible with our findings if we keep in mind that the authors found the same apoptotic macroglial cells in newborn mice. We found apoptotic profiles in nearly all the macroglial cells; therefore it can be suggested that an apoptotic process is activated in $P27^{Kip1}$ deficient mice affecting the axonal myelin. This observation is consistent with the proposal that as development progressed, the proportion of apoptotic nuclei increased, as we observed in our 26-week-old mice.

Some authors explain this apoptotic hypothesis as a secondary cause of the increase in the number of macroglial cells, which would affect the axonal contact, which determines the number of oligodendrocytes and astrocytes, eliminating these by programmed cell death (19, 20). On the other hand, it is more plausible to think of a generalized apoptotic process as it is demonstrated by the presence of apoptotic retinal ganglion cells in $P27^{Kip1}$ -/- mice documented by TUNEL assay (10), and this hypothesis would also explain the severe intra-axonal degeneration present in our axons.

To summarize, we propose two hypotheses to explain our results: on the one hand, a development impairment of the myelination process, and on the other, an apoptotic process leading to a severe degeneration in the axons and myelin.

Taken together, our results suggest that homozygous $P27^{Kip1}$ knockout mice showed hypertrophic ON with ultrastructural abnormalities and axonal hyperplasia, by mechanisms not fully understood that are our main goal for future studies, including TUNEL techniques.

Proprietary interest: None.

Reprint requests to:
Enrique López-Sánchez, MD
Gran Vía Germanías 45 p-31
Valencia 46006, Spain
elopez@comv.es

REFERENCES

1. Tong W, Pollard JW. Genetic evidence for the interactions of cyclin D1 and P27^{Kip1} in mice. Mol Cell Biol 2001; 21: 1319-28.
2. Lee WH, Shew JY, Hong FD. The retinoblastoma susceptibility gene encodes a nuclear phosphoprotein associated with DNA binding activity. Nature 1987; 329: 642.
3. Lundberg AS, Weinberg RA. Functional inactivation of the retinoblastoma protein requires sequential modification by at least two distinct cyclin Cdks complex. Moll Cell Biol 1998; 18: 753-61.
4. Harbour JW, Luo RX, Dei Santi A, et al. Cdk phosphorylation triggers sequential intramolecular interactions that progressively block Rb functions as cells move through G1. Cell 1999; 98: 859-69.
5. Weng LP, Brown JL, Eng C. PTEN coordinates G1 arrest by down-regulating cyclin D1 via its protein phosphatase activity and up-regulating p27 via its lipid phosphatase activity in a breast cancer model. Hum Mol Genet 2001; 10: 599-604.
6. Foster JS, Henley DC, Bukovsky. Multifaceted regulation of cell cycle progression by estrogen: regulation of Cdk inhibitors and Cdc25A independent of cyclin D1-Cdk4 function. Mol Cell Biol 2001; 21: 794-810.
7. Nakayama K, Ishida N, Shirane M, et al. Mice lacking p27(Kip1) display increased body size, multiple organ hyperplasia, retinal dysplasia, and pituitary tumors. Cell 1996; 85: 707-20.
8. Egerton M, Scollay R, Shortman K. Kinetics of mature T-cell development in the thymus. Proc Natl Acad Sci USA 1990; 87: 2579-582.
9. Jacks T, Fazeli A, Schmitt EM, et al. Effects of an Rb mutation in the mouse. Nature 1992; 359: 295-300.
10. Dyer MA, Cepko CL. P27^{Kip1} and p57^{Kip2} regulate proliferation in distinct retinal progenitor cell populations. J Neurosci 2001; 12: 4259-71.
11. Casaccia-Bonnefil P, Tikoo R, Kiyokawa H, et al. Oligodendrocyte precursor differentiation is perturbed in the absence of the cyclin-dependent kinase inhibitor p27^{Kip1}. Genes Dev 1997; 11: 2335-46.
12. Miskimins R, Srinivasan R, Main-Husstege M, et al. P27^{kip1} enhances myelin basic protein gene promoter activity. J Neurosci Res 2002; 67: 100-5.
13. Pinazo-Durán MD, Renau-Piqueras J, Guerri C. Developmental changes in the optic nerve related to ethanol consumption in pregnant rats: analysis of the ethanol-exposed optic nerve. Teratology 1993; 48: 305-22.
14. López-Sánchez E, Francés-Muñoz E, Díez-Juan A, Andrés V, Menezo JL, Pinazo-Durán MD. Optic nerve alterations in apolipoprotein E deficient mice. Eur J Ophthalmol 2003; 13: 560-5.
15. Pinazo-Durán MD, Cervera R, Pons S, Zanón-Moreno VC, Gallego-Pinazo R, Guerri C. Mechanisms of protein expression in the rat optic nerve. Modifications by alcohol exposure. Arch Soc Esp Oftalmol 2005; 80: 99-104.
16. Williams BO, Schmitt EM, Remington L, et al. Extensive contribution of Rb-deficient cells to adult chimeric mice with limited histopathological consequences. EMBO J 1994; 13: 4251-9.
17. Noble M, Murray K, Stroobant P, et al. Platelet-derived growth factor promotes division and motility and inhibits premature differentiation of the oligodendrocyte/type-2 astrocyte progenitor cell. Nature 1998; 333: 556-62.
18. Miskimins R, Knapp L, Dewey MJ, et al. Cell and tissue-specific expression of a heterologous gene under control of the myelin basic protein gene promoter in transgenic mice. Brain Res Dev Brain Res 1992; 65: 217-21.
19. Burne JF, Staple JK, Raff MC. Glial cells are increased proportionally in transgenic optic nerves with increased numbers of axons. J Neurosci 1996; 16: 2064-73.
20. Raff MC, Barres BA, Burne JF, Coles HS, Ishizaki Y, Jacobson MD. Programmed cell death and the control of cell survival: lessons from the nervous system. Science. 1993; 262: 695-700.